NGI Teknisk notat

Til:	Norges vassdrags- og energidirektorat
v/:	Aart Verhage
Kopi til:	
Dato:	2017-02-03
Rev.nr. / Rev.dato:	0/
Dokumentnr.:	20140053-03-TN
Prosjekt:	FoU Snøskred 2014–2016 WP 1
Prosjektleder:	Peter Gauer
Utarbeidet av:	Dieter Issler
Kontrollert av:	Peter Gauer

Notes on Fluidization of Snow Avalanches by Air Expulsion From the Snow Cover

Sammendrag / ***Abstract***

A recently proposed mechanism for fluidization of the front of dry-snow avalanches, based on air escaping from the snow cover that is compressed under the weight of the avalanche (Issler, 2013), is discussed. A minimal set of governing equations for a quasi-3D depth-averaged flow model is developed and some possible extensions to this scheme are presented. The model requires a number of constitutive relations describing (i) the rate of compression of the snow cover under simultaneous sudden application of shear and normal stress, (ii) the permeability of the snow cover and the avalanche body as a function of density and possibly particle granulometry, and (iii) the reduction of the effective stress in the avalanche body due to the escaping air. The model lends itself to integration with both basal and frontal entrainment models (Issler, 2014; Gauer and Issler, 2004), and to an extension describing the formation of a suspension layer. This is a report on work in progress; it will be revised and extended as the work progresses.

Innhold / *Table of Contents*

1 Introduction

Field observations indicate that snow avalanches can reach a fluidized flow regime at moderate velocities on relatively gentle slopes and maintain it for long distances even in the run-out zone in some cases. This appears to exclude inter-particle collisions and aerodynamic underpressure behind the nose as sufficient fluidization mechanisms. Avalanche mobility also varies strongly between events with similar release masses in the same path, pointing towards a more significant role of the substrate, i.e., the snow cover, in the dynamics of snow avalanches than hitherto recognized.

Excess pore pressure is a key concept in the description of all types of landslides, both subaerial and subaqueous. It is therefore somewhat surprising that it has not been applied to snow avalanches, given the many similarities avalanches share with earth flows. An explanation may be that the pore fluid in snow avalanches is air, which is perceived as too compressible and light relative to the ice crystals. In contrast, the pore fluid in mudflows and debris avalanches is water, whose density is constant and comparable to that of the solid component.

Gauer and Issler (2004) hypothesized that compression of the pore air in the snow cover by the avalanche flowing over it could be pressed out just right in front of the avalanche head and carry the (least consolidated) top layer with it. Louge and coworkers (Louge and others, 2011; Carroll and others, 2012, 2013) applied this concept to powder-snow avalanches, calling it eruption currents. They focused, not on the overpressure due to the weight of the dense flow, but the underpressure aerodynamically created in front of the approaching avalanche (Nishimura and others, 1995; McElwaine and Nishimura, 2001; McElwaine, 2005; McElwaine and Turnbull, 2005; Turnbull and McElwaine, 2008). In this way, they derived expressions for the erosion rate.

During a discussion on the reasons for abnormally low effective friction angles for some snow avalanches at the GeoFlow 13 workshop, Mohrig (personal communication, 2013) pointed out that the substrate, i.e., the snow cover, most likely played a decisive role in this phenomenon. Elaborating on this suggestion, the author proposed a conceptual model for fluidization (Issler, 2013) that builds on the concept of air expulsion from (Gauer and Issler, 2004), but recognizes that most of the air squeezed out of the snow cover will flow through the avalanche body itself and support its fluidization. The following processes are deemed to be relevant for this effect:

- The texture of the new-snow layer is destroyed rapidly due to shear and normal loads when it is overflowed by the avalanche. The new-snow layer nevertheless has a residual strength that increases as it gets compacted.
- The compaction rate is limited by how quickly the pore air can be pressed out. This time scale depends on the pressure gradient due to the overburden and the permeability of the snow cover and the avalanche.

- As the pore air escapes, it exerts an upward force onto the avalanche, i.e., the effective pressure and the concomitant frictional shear stress diminish. Complete fluidization cannot be achieved in this way, however.
- An additional mechanism—presumably dispersive pressure from grain–grain collisions and/or aerodynamic underpressure—must be invoked to complete fluidization and to lift the snow enough to obtain the observed intermediate densities of fluidized avalanches.

From this concept, we expect that complete fluidization is usually only possible as long as pore air is expelled from the new-snow layer, i.e., only the frontal part of the avalanche will be fluidized. Frictional shear stress is reduced significantly in the fully fluidized head, which will therefore flow at higher speed and achieve a longer run-out. The degree of fluidization and the length of the fluidized zone depend critically on the depth and permeability of the snow cover and the avalanche.

The objective of the present note is to discuss this fluidization mechanism critically and to formulate it more quantitatively in a form that is amenable to implementation in a numerical model. Section 2 discusses how much the new-snow layer can be compressed and what this implies for the excess pore pressure. In Sec. 3, the focus is on the speed at which pore air is expelled from the new-snow layer and the avalanche. We consider possible equations to describe the density evolution of the avalanche in Sec. 4 before outlining the remaining work in Sec. 5.

2 Compressibility of the snow cover, effective pressure and fluidization

As the avalanche front propagates, the snow cover that is being overflowed is suddenly exposed to normal stresses of the order of 1–10 kPa and shear stresses roughly half that size. The extra normal load will inevitably lead to some compression of the snow cover. For loads near the lower end of this range, there will be only slight compression of well settled old-snow layers, but a new-snow layer overflowed by a substantial avalanche exerting 1 kPa or more of shear stress and some 2 kPa of normal stress is expected to break up into small fragments. The loading is very rapid, and the stresses are of a magnitude that brings the snow into the brittle-fracture regime.

Typical new-snow densities are 100–200 $\mathrm{kg\,m^{-3}}$, i.e., the volumetric particle concentration is only 0.1–0.2 while the voidage is 0.8–0.9. This makes new snow an extremely contractive material. The density of the new-snow layer right after the avalanche event depends on the initial density and the extra load from the flow. There are a few field observations where the density of the snow cover underneath an avalanche deposit was measured and compared to the values measured in the undisturbed snow cover outside the avalanche perimeter. These measurements indicate typical compressed densities in

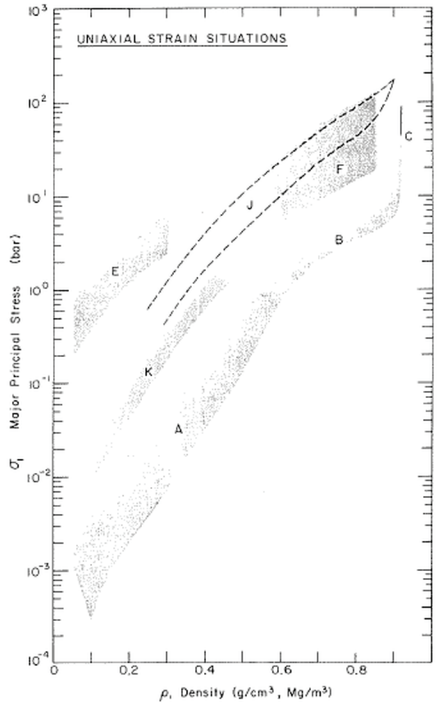

Figure 1 Normal-stress–density relations for different types of snow and ice under different loading conditions. From (Mellor, 1975). The relation K from uniaxial loading until fracture appears most appropriate to compression of the new-snow layer under the weight of an avalanche.

the range 200–300 kg m^{-3}, i.e., about 50–100% higher than the initial density. Typically, the depth of the new-snow layer is reduced by 0.1–0.5 m, i.e., between 0.1 and 0.5 m^3 of air (at ambient pressure) per square meter have to escape from the new-snow layer.

There are few studies of the compressibility of snow, and perhaps even fewer that apply to natural new snow. The most relevant experimental data appears to be collected in (Mellor, 1975, Fig. 13), which is reproduced here as Fig. 1, and in (Abele and Gow, 1975). Natural snow settling under its own weight will reach densities of 200–300 kg m^{-3} and 400–500 kg m^{-3} under normal stresses of 1 kPa and 10 kPa, respectively. Under incremental loading to failure under uniaxial strain, the same loads achieve final densities of only about 120 and 270 kg m^{-3}, respectively. Virtually no compression would be obtained by means of an impact load of 10 kPa according to the theoretical model by Mellor (1968). The latter calculation assumes that the pore air cannot escape (undrained conditions in geotechnical terminology) and therefore does not apply to our situation. Natural compaction occurs over a period of months and thus likely overestimates the compaction over a few seconds significantly. Mellor does not mention whether the uniaxial compression tests were carried out at drained or undrained conditions, but drained conditions are more plausible. Thus this intermediate normal load–density relation likely is the most realistic in the present context. In the range of interest (1–10 kPa), it may be approximated

as

$$\rho(\sigma_n) \approx \left(100 + 170 \lg \frac{\sigma_n}{1\,\mathrm{kPa}}\right) \mathrm{kg\,m^{-3}}. \tag{1}$$

It is as yet unclear how large the natural variability between different types of new snow is.

The role of the pore air in the compression of snow needs to be discussed briefly. At the scale of ambient pressure, ≈ 100 kPa, air is highly compressible. However, the stresses inside an avalanche or snow cover are one to two orders of magnitude smaller. Under gravity-induced compaction of snow, the pore air thus behaves like a nearly incompressible liquid. The excess pore pressure (the difference between the air pressure in the pores, p_a, and the ambient pressure, p_{amb}) may reach values of a few kilopascal. This provides the pressure gradient that presses pore air out, but changes the air density by at most a few per cent. Consequently, we may approximate the air density as constant. This effective incompressibility of the air prevents the snow cover overflowed by an avalanche from being compacted at once; instead, the compaction is governed by the rate at which air can flow out to dissipate the excess pore pressure.

Next consider the effect of the escaping air on the snow-particle skeleton. Only a tiny fraction of the excess pore pressure is consumed by accelerating the air, the rest is available for overcoming the flow resistance due to pressure drag and friction drag. The pressure drag arises from the pressure difference between the lower and upper sides of protrusions or cavities in the wall of the "pipes" through which the air escapes. The friction drag is due to viscous shear stress along the "pipe" walls. Neglecting the small amount of kinetic energy of the escaping pore air, the balance of momentum implies that the net slope-normal traction on the avalanche be equal to the pore pressure drop between the bottom and top of the avalanche, multiplied by the fraction of the cross-section occupied by pores. The latter is equal to the volume fraction of pores (or the voidage). This slope-normal traction reduces the effective pressure, p_e, i.e., the normal stress transmitted through persistent inter-particle contacts, but not p_d, the dispersive pressure from collisions, which is a function of the shear rate and the density.

If we assume the density and permeability to be constant across the depth of the avalanche and inertial effects to be small, the force balance in the slope-normal direction at a distance z from the flow surface is

$$\begin{aligned} \rho g_z z &= p_e(z) + p_d(z) + (p_a(z) - p_{\mathrm{amb}})(1 - c_f) \\ &= p_e(z) + p_d(z) + p_u(z). \end{aligned} \tag{2}$$

From here on, the subscripts f, s, a and 'amb' will denote quantities related to the flowing avalanche, the snow cover, the pore air and the ambient air, respectively, if there is need for distinction. Accordingly, c_f is the volume concentration of snow particles in the avalanche and h_f is the flow depth. Note that the effective, dispersive and bulk excess pore pressure, p_u, all refer to the bulk, whereas p_a is the thermodynamic pressure of the

pore air, whence the factor $1 - c_f$. Solving for p_e gives

$$p_e(z) = \left[\rho_f g_z h_f - p_u(h_f)\right] \frac{z}{h_f} - p_d(z). \tag{3}$$

Thus the excess pore pressure reduces the effective pressure inside the flowing avalanche and the Coulomb-type friction forces, but not the shear stress due to particle collisions.

An important point is that the bulk excess pore-pressure cannot be larger than the overburden from which it arises. In the new-snow layer, we can use eq. (2) to determine p_u if we make assumptions on p_e. In the snow cover, $p_d = 0$ and p_e can be identified with the residual strength of the ice skeleton during collapse. The simultaneous action of shear and normal stresses suggests that the bonds between the snow grains are broken almost instantaneously so that the material becomes a contractive granular material. Under these circumstances, one may expect Coulomb-like behavior under failure. In many cases, the particles are not spherical, but of dendritic shape so that the coordination number (the average number of contacts a particle has) is quite high at low bulk density. However, under shear these delicate feathery extensions are easily broken and force chains are interrupted. Under these conditions, we expect the effective friction coefficient to be significantly smaller than for granular materials of nearly spherical particles. Conversely, if the dendritic crystals are very strong, their shape will lead to a large friction coefficient μ_b. Thus we make the assumption

$$p_e(z) = \mu_b g_z[\rho_f h_f + \rho_b(z - h_f)] \tag{4}$$

and conjecture $0.2 < \mu_b < 0.4$ if the dendritic crystals break, and $0.5 < \mu_b < 0.8$ if they do not break. μ_b is expected to grow as the density of the new-snow layer and thus the coordination number increases.

3 Permeability of the snow cover and the flowing avalanche

The preceding discussion implies that p_u (and thus p_e) at a given instant does not directly depend on how fast the pore air escapes. Conversely, the escape rate depends directly on p_u. The more slowly the pore air escapes and the larger the expelled volume of pore air, the longer will the fluidized head of the avalanche be. The air flow rate, in turn, depends on the permeability and depth of the new-snow layer and the avalanche. While some air can be pressed into the underlying old-snow layers or escape along the circumference of the avalanche body, we will neglect these effects here.

The rate at which air seeps through the avalanche body, q_a ($\mathrm{m\,s^{-1}}$), is governed by the pore pressure gradient, $\partial_z p$, the specific permeability of the avalanche body, K ($\mathrm{m^2}$), and

the dynamic viscosity of air[1], η_a (Pa s):

$$q_a = -\frac{K}{\eta_a}\partial_z p_u. \tag{5}$$

The pore pressure gradient is given, to first approximation, by the ratio of excess pore air pressure at the interface, $p_u(h_f)$, and the avalanche flow depth, h_f. The permeability must be estimated from the avalanche density and the likely particle size distribution.

As a first step, we estimate the specific permeability of typical new-snow layers and avalanche flows. Shimizu (1970) carried out a comprehensive study on natural snow at different stages of metamorphosis and proposed a formula for the specific permeability of fine-grained snow. He found values between 1.5–3 times smaller than in earlier studies. Domine and others (2013) studied (subarctic) seasonal snow and found that the formula

$$K = 3.0\, r^2 \mathrm{e}^{-0.013 \mathrm{m^3\,kg^{-1}} \rho} \tag{6}$$

gives a much better approximation for new snow than Shimizu's. Both authors agree, however, on the point that specific permeability diminishes exponentially with density, ρ, as the pores become smaller relative to the grains. The quantity r is the equivalent sphere radius, determined from the surface area per unit volume, SSA_V, by

$$r = \frac{3}{\mathrm{SSA}_V}. \tag{7}$$

The equivalent sphere radius of new snow is $r = O(10^{-4}\,\mathrm{m})$ while fine-grained snow has $r \approx 4 \times 10^{-4}\,\mathrm{m}$. Typical values of the permeability of new snow with density in the range 100–200 $\mathrm{kg\,m^{-3}}$ are (0.3–1) $\times\, 10^{-8}\,\mathrm{m^2}$ due to the very irregular surface structure that creates much shear. Fine-grained snow with roughly double the density of new snow has similar permeability because the particles are more rounded and the pore walls therefore are smoother. The permeability of layers of depth hoar or faceted crystals, which typically are significantly larger, can be more than an order of magnitude larger. (Note that Domine and others (2013) did not investigate snow denser than 240 $\mathrm{kg\,m^{-3}}$.)

The permeability of flowing avalanches cannot readily be measured and therefore must be estimated—with large uncertainty. Presumably it varies by orders of magnitude in the course of the event and also between different locations in the avalanche (head vs. tail, surface vs. bottom). The large particles present in the non-suspended part of the avalanche are permeable themselves to some degree, but we will ignore this for the time being and focus on the matrix of fine particles that fill the space between the large particles. For the sake of simplicity, we consider all particles less than 1–2 mm in diameter as small and the remainder as large. From field observations, we estimate that small particles represent a fraction $0.5 < s < 0.9$ of the total particle volume fraction c_f in a dry-snow avalanche. (However, we have observed highly granular wet-snow avalanches where large particles 5–20 cm in diameter accounted for nearly the entire mass.)

[1] If the air flow carries along fine snow particles, the mixture may have a significantly higher viscosity.

The intrinsic density of small particles is close to the density of ice (917 kg m^{-3}), whereas large particles have typical densities in the range $\rho_p = 300$–$500\,\mathrm{kg\,m^{-3}}$. The density of the mixture of air, large and small particles is $\rho \approx [(1-s)\rho_p + s\rho_i]c_f$. The large particles thus block a volume fraction $(1-s)c_f$ from seepage flow, while small particles fill the fraction $sc_f/[1-(1-s)c_f]$ of the remaining space. A rough estimate for the specific permeability then is

$$K_f \approx [1-(1-s)c_f]K(\rho'), \tag{8}$$

where $K(\rho')$ is obtained from Eq. (6) by setting $\rho' = \rho_i \frac{sc_f}{1-(1-s)c_f}$. The equivalent sphere radius of the small particles should be similar to that in the new-snow layer, i.e., $r \approx 10^{-4}$ m, unless the avalanche has entrained large amounts of older or humid snow. $K(\rho')$ will have similar values as in the new-snow layer, and the factor in square brackets in Eq. (8) is usually between 0.7 and 1. From this we tentatively infer that the permeability in the flowing avalanche may be slightly lower than in the new-snow layer. It appears reasonable to assume K is about the same as in the new-snow layer as long as the avalanche is not fully fluidized, but that K increases significantly as the avalanche density decreases.

As an avalanche becomes fluidized, the permeability increases significantly. Formula (8) gives $K = 0.22 \times 10^{-8}\,\mathrm{m^2}$ for an avalanche of density $200\,\mathrm{kg\,m^{-3}}$ consisting of new snow with $r = 10^{-4}$ m, but $K = 1.57 \times 10^{-8}\,\mathrm{m^2}$ if the density has dropped to $50\,\mathrm{kg\,m^{-3}}$. Granulation (Steinkogler and others, 2014) has an even more dramatic effect as r^2 may increase by four to six orders of magnitude.

One needs to take into account that the seepage flow may be non-Darcian, with the flow rate increasing sub-linearly with the pressure gradient due to turbulence developing in the pore flow. This effect can be quite pronounced so that the effective permeability and thus the seepage rate may be one to two orders of magnitude smaller than one would expect for Darcian flow. In snow avalanches, this difference may have (literally) far-reaching consequences.

The pore air pressure gradient and the permeability in the avalanche determine the air flux across the flow depth. However, Darcy's law may not be adequate in this situation because the flow in the pores will often be turbulent: For an order-of-magnitude estimate, assume a new-snow layer of initial depth $h_{b,0} = 0.5$ m and initial density $\rho_{b,0} = 150\,\mathrm{kg\,m^{-3}}$ to be compressed to the final density $\rho_{b,1} = 300\,\mathrm{kg\,m^{-3}}$ and that the pore pressure equilibrates over $\Delta t = 5$ s. This gives an average bulk air flow velocity of

$$\bar{v}_{a,\mathrm{bulk}} = \frac{h_{b,0}}{\Delta t} \cdot \frac{\rho_{b,0}}{\rho_{b,1}} = 0.05\,\mathrm{m\,s^{-1}}.$$

For volumetric snow-particle concentrations in the avalanche in the range $0.2 < c_p < 0.6$, the average air flow speed in the pores then becomes

$$\bar{v}_{a,\mathrm{pore}} = \bar{v}_{a,\mathrm{bulk}} \cdot \frac{1}{1-c_p} = 0.06\text{–}0.12\,\mathrm{m\,s^{-1}}. \tag{9}$$

The resulting Reynolds number depends strongly on the pore diameter, d_{pore}, which one expects to vary between roughly 0.001 m and 0.1 m. One then arrives at

$$\text{Re} = \frac{\bar{v}_{a,\text{pore}} d_{\text{pore}}}{\nu_a} \approx 10^0\text{–}10^3. \tag{10}$$

Thus the air flow in the pores is expected to be laminar or nearly laminar in dense, small-grained avalanches and turbulent in strongly fluidized avalanches with many large particles.

In fluidized avalanches with densities below approx. 100 kg m^{-3}, the snow particles will not be in permanent contact. This makes it possible to roughly estimate the effective permeability and the influence of turbulence by boldly treating the particles as isolated and calculate the pressure gradient from the drag force. Assume the avalanche density and flow depth to be ρ_f and h_f, respectively, while the particles have intrinsic density ρ_p, average exposed diameter d and drag coefficient C_D. If the bulk flow velocity is $\bar{v}_{a,\text{bulk}}$, the excess pore pressure gradient is

$$\begin{aligned} \partial_z p_u &\approx n_p \frac{1}{2} C_D(\text{Re}_p) d^2 \rho_a \bar{v}^2_{a,\text{pore}} \\ &\approx \frac{1}{2} C_D(\text{Re}_p) d^2 \frac{\rho_f}{\rho_p d^3} \rho_a \bar{v}^2_{a,\text{bulk}} \left(\frac{1}{1-\rho_f/\rho_p} \right)^2 \\ &= \frac{1}{2} C_D(\text{Re}_p) \frac{\bar{v}_{a,\text{bulk}}}{d} \frac{\rho_f \rho_p}{(\rho_p - \rho_f)^2} \rho_a \bar{v}_{a,\text{bulk}} \end{aligned} \tag{11}$$

This expression leads to an effective permeability that depends on the particle Reynolds number, $\text{Re}_p \equiv \rho_a \bar{v}_{a,\text{bulk}} d/\eta_a$, of the snow particles in the seepage flow:

$$K_{\text{eff}} = \frac{2}{C_D(\text{Re}_p)\text{Re}_p} \frac{(1-c)^2}{c} d^2. \tag{12}$$

The factor d^2 reflects the fact that the pore size grows with particle size. K_{eff} vanishes quadratically as the pore space goes to zero ($c \to 1$) and diverges as the particle concentration or density goes to zero ($c \to 0$). For low Re_p, $C_D \propto 1/\text{Re}_p$, thus K_{eff} is independent of Re_p. At high Re_p, C_D becomes independent of Re_p and $K_{\text{eff}} \propto 1/\text{Re}_p$.

4 Density evolution of the avalanche

The collapse of the snow cover under the weight of the avalanche flowing over it creates a pressure difference across the depth of the avalanche body that is roughly proportional to, but smaller than, the overburden due to the residual frictional resistance of the snow cover against compression. By itself, the pore pressure gradient in the avalanche can only achieve partial fluidization, but this will nevertheless reduce the (Coulomb-type) shear stress opposing the avalanche flow. Accordingly, the avalanche will flow more rapidly

so that the dispersive shear and normal stresses will increase. In parallel, the density of the avalanche diminishes. Granular flow experiments (MiDi, 2004) indicate that the density decreases about linearly with the so-called inertial number and thus with the shear rate. The avalanche can attain the state of total fluidization, in which the effective stress vanishes, if the dispersive normal stress and the underpressure due to the air flow over the avalanche can compensate the remaining effective pressure:

$$\begin{aligned} p_e(h_f) &= h_f \rho g \cos\theta - p_u(h_f) - \frac{1}{2} C_L \rho_a U^2 \\ &= \begin{cases} 0, & \text{total fluidization,} \\ > 0, & \text{partial fluidization.} \end{cases} \end{aligned} \tag{13}$$

We will not discuss the aerodynamic underpressure further in this note; see (Issler and Gauer, 2008) for additional remarks.

Next, we need to address the question how excess pore pressure and dispersive pressure determine the density of the completely fluidized avalanche in a stationary flow. The excess pore pressure, being proportional to the overburden, is in first approximation independent of the avalanche density (however, the permeability and thus the flow rate depend strongly on the density). The dispersive pressure and shear stress, in contrast, exhibit a very pronounced dependence on the density (Issler and Gauer, 2008). Consider a quasi-stationary flow on an incline, with slope angle θ, m the mass per unit footprint area, $g_z \equiv g\cos\theta$ and $g_x \equiv g\sin\theta$ the components of gravitational acceleration. Assume that the density is uniform across the depth of the avalanche, $h_f = m/\rho_f$, and that the excess pore pressure is a fraction r of the overburden, i.e., $p_u(z) = -rmg_z z/h_f = -r\rho g_z z$. The extended NIS model (Issler and Gauer, 2008) specifies the stresses σ_{zz} and σ_{xz} as

$$\sigma_{zz}(z) = p_e(z) + p_u(z) + \rho\nu_n(\rho)\dot{\gamma}^2(z) \stackrel{!}{=} \rho g_z z, \tag{14}$$

$$\sigma_{xz}(z) = \mu p_e(z) + \rho\nu_s(\rho)\dot{\gamma}^2(z) \stackrel{!}{=} \rho g_x z. \tag{15}$$

As we assume the excess pore pressure and the dispersive pressure combined to be strong enough to support the overburden (i.e., $p_e = 0$), we obtain from eq. (15) that

$$\nu_s(\rho)\dot{\gamma}^2(z) = g_x z,$$

which can be inserted in eq. (14) to obtain

$$\frac{\nu_s(\rho)}{\nu_n(\rho)} = \frac{g_x}{(1-r)g_z} = \frac{\tan\theta}{1-r}. \tag{16}$$

Thus, once the density dependence of ν_n and ν_s is specified, the equilibrium density for a given slope angle and the value of r can be determined. Then also the shear rate $\dot{\gamma}(z) = \sqrt{zg_x/\nu_s(\rho)}$ and the depth-averaged velocity can be calculated (the velocity profile is Bagnoldian in this model).

Now consider the situation of partial fluidization where $p_e(z) > 0$. There are three unknowns, i.e., p_e in addition to ρ and $\dot{\gamma}$, but only two equations. Equation (14) gives

$$p_e(z) = (1-r)\rho g_z z - \rho \nu_n \dot{\gamma}^2(z).$$

Applying this to eq. (15) leads to

$$\dot{\gamma}^2(z) = z\frac{g_x - (1-r)\mu g_z}{\nu_s(\rho) - \mu\nu_n(\rho)},$$

where ρ remains undetermined. Two possible assumptions supplying the missing condition are the following: (i) As in (Issler and Gauer, 2008), the density is assumed to be constant until the conditions for full fluidization are met. One sets $\rho = \rho_0$ and can then solve for $\dot{\gamma}(z)$ as usual. (ii) One adopts the relation known from the $\mu(I)$ rheology,

$$c(z) = c_{\max} - (c_{\max} - c_{\min})\, I(z), \tag{17}$$

where the inertial number is defined by $I(z) \equiv \dot{\gamma}(z)d/\sqrt{zg_z}$ and d is the mean particle diameter. Typical values for the volumetric concentrations are $c_{\min} \approx 0.5$ and $c_{\max} \approx 0.6$, corresponding to avalanche densities $\rho_{\min} \approx 150$–$250\,\mathrm{kg\,m^{-3}}$ and $\rho_{\max} \approx 200$–$300\,\mathrm{kg\,m^{-3}}$.

Alternative (ii) is the more physical approach because shearing of a dense granular mass leads to dilation. However, it is unclear by how much $c_{\min}$ and $c_{\max}$ have to be increased to account for the wide distribution of particle sizes in snow avalanches. Moreover, the formula (17) is linked to the $\mu(I)$ rheology, which behaves quite differently from the NIS rheology. For these reasons, we provisionally adopt approach (i). Issler and Gauer (2008) obtained curves for $\nu_{n,s}(c)$ by approximating results from 2D calculations in kinetic theory (Pasquarell and others, 1988) and 2D DEM simulations (Campbell and Gong, 1986):

$$\nu_n(c) = Ac^{-p}(c_* - c)^{-q}, \tag{18}$$
$$\nu_s(c) = k\nu_n(c)\,(1 + bc^{-s})\,. \tag{19}$$

Typical values of the parameters are $c_* = 0.6$ and $A = 10^{-4}\,\mathrm{m^2}$ for a grain diameter of 1 cm. The values $b = 1$, $k = 0.2$, $p = 0.5$, $q = 1.5$, and $s = 0.5$ give a fairly good approximation of the theoretical curves. These curves ought to be updated to reflect more recent 3D simulations, but we will nevertheless use them for demonstrating the basic features of the model.

Finally, we need to address the question of the dynamics of the avalanche motion in the z-direction. A possible starting point is the z-component of the momentum balance equation,

$$\partial_t(\rho_f w) + \nabla_\parallel \cdot (\rho_f w \boldsymbol{u}_\parallel) + \partial_z(\rho_f w^2) = \partial_i \sigma_{zi} + \rho_f g_z,$$

where the velocity is decomposed as $\boldsymbol{u} \equiv (\boldsymbol{u}_\parallel, w)^T$, the z-coordinate is measured from the avalanche surface downward, and summation is implied over the repeated index i. The

boundary conditions are $w(x, y, h_f, t) = 0$ (no vertical velocity at the ground, provided there is no erosion) and $\sigma_{iz}(x, y, 0, t) = 0$, i.e., the surface is stress-free. This equation can be integrated over z to give

$$\partial_t(h_f\bar{\rho}_f\bar{w}) + \nabla_\parallel \cdot (f_{uw}h_f\bar{\rho}_f\bar{w}\bar{\boldsymbol{u}}_\parallel) + \bar{\rho}_f w_s^2 = \nabla_\parallel \cdot (h_f\bar{\boldsymbol{\sigma}}_{z\parallel}) - \sigma_{zz}(h_f) + h_f\bar{\rho}_f g_z. \quad (20)$$

Here, $w_s \equiv w(x, y, 0, t)$ is the bed-normal velocity at the avalanche surface. In order to proceed, we make two (mutually compatible) assumptions: (i) The density is uniform across the avalanche depth, i.e., $\rho(x, y, z, t) = \bar{\rho}(x, y, t)$. (ii) The vertical velocity w grows linearly from the bed to the surface so that $w_s = 2\bar{w}$. If one assumes a Bagnold profile for $\bar{\boldsymbol{u}}$ (as predicted by the extended NIS rheology), the form factor evaluates to $f_{uw} = 9/7$. For the normal stress at the bed, $\sigma_n^{(b)} \equiv \sigma_{zz}(h_f)$, the extended NIS model gives $\sigma_n^{(b)}$ as the sum of excess pore pressure and dispersive normal stress,

$$\sigma_n^{(b)} = r\rho g_z h_f + \frac{25}{4}\nu_n(\rho)\rho\left(\frac{\bar{\boldsymbol{u}}_f}{h_f}\right)^2, \quad (21)$$

in the case of total fluidization ($p_e = 0$). If fluidization is only partial, $\sigma_n^{(b)}$ must equal the overburden $\rho g_z h_f$, and the effective pressure at the bed–flow interface is $p_e^{(b)} = (1 - r)\rho g_z h_f - (25/4)\nu_n(\rho)\rho(\bar{\boldsymbol{u}}_f/h_f)^2$.

In order to close eq. (20), we need to specify the ratio of excess pore pressure to overburden, r. To this end, the dynamics of pore pressure creation by compression of the snow cover and pore pressure dissipation by air flow through the avalanche needs to be captured. Assuming isotropic permeability across the depth of the avalanche, we obtain the air flow rate across h_f from eq. (6) as

$$q_a = -\frac{K_{\text{eff}}}{\eta_a}\frac{p_u}{h_f}.$$

We can use this expression in a balance equation for the air in the snow cover:

$$\frac{\mathrm{d}}{\mathrm{d}t}(h_s\rho_a c_a) = \rho_a q_a,$$

where h_s is the depth of the (new-)snow layer and c_a the volume fraction of air in the snow. The latter can be expressed as $c_a \approx 1 - \rho_s/\rho_i$ in terms of the densities of the snow layer and solid ice, respectively. The air density inside the snow cover depends on the air pressure inside the snow cover, which can be expressed in terms of the excess pore pressure if we assume isothermal compression of an ideal gas:

$$\rho_a = \rho_{\text{amb}}\frac{p_a}{p_{\text{amb}}} = \rho_{\text{amb}}\frac{p_u}{c_a p_{\text{amb}}}.$$

The subscript ‘amb’ refers to the undisturbed ambient air. Expressing ρ_a through the excess pore pressure and the snow-cover density, we arrive at the ordinary differential equation

$$\frac{\mathrm{d}}{\mathrm{d}t}\left(\frac{h_s p_u}{\rho_i - \rho_s}\right) = -\frac{K_{\text{eff}}}{\eta_a}\frac{p_u}{h_f}\frac{p_u}{\rho_i - \rho_s}. \quad (22)$$

If we consider a situation where the snow density and snow depth are artificially held constant, eq. (22) simplifies to $\dot{p}_u = -Cp_u^2$, i.e., the excess pore pressure drops like $p_u(t) \propto 1/t$. Mass conservation implies $h_s(x,y,t) = h_{s,0}(x,y)\rho_{s,0}(x,y)/\rho_s(x,y,t)$ if we neglect the mass of the pore air and snow erosion. Equation (22) can thus be expressed in terms of p_u, $\dot{p}_u$, ρ_s and $\dot{\rho}_s$.

We assume that the relaxation of the snow cover following a change in pressure is very fast so that the density effectively is the equilibrium density corresponding to the instantaneous effective stress state, $\rho_s(p_e)$, cf. eq. (1). The momentum balance in z-direction for the snow cover leads to

$$p_e^{(b)} = \rho_f h_f (g_z - \dot{\overline{w}}) - p_u^{(b)},$$

with the second term in parentheses accounting for inertial forces. If we can neglect the inertial term in this equation, we directly obtain ρ_s as a function of p_u and $\dot{\rho}_s$ as a function of p_u and $\dot{p}_u$. Therewith eq. (22) becomes a closed equation for pore pressure evolution.

In shallow-water or depth-averaged models, it is important to truncate the equations consistently with regard to the relevant time scales. Gravity-driven waves should be taken into account in these models, but disturbances propagating at the speed of sound in the flowing medium typically traverse the depth of the flow much faster than the flow in its entirety reacts to, e.g., a change of slope inclination. Unless second-order effects like deviations of the velocity profile from the equilibrium shape are also taken into account, the fast modes of vertical motion should be filtered out (Issler and others, 2017). One way to achieve this is to use the instantaneous equilibrium values of the density and the flow depth and to reduce the momentum balance in bed-normal direction to the equation for hydrostatic equilibrium. The density at a given location and time is determined from eq. (21) by setting $\sigma_n^{(b)} = \rho g_z h_f$ and substituting $h_f = m/\rho$, with m the flow mass per unit footprint area. This leads to

$$\nu_n(\rho)\rho^3 = \frac{4}{25}(1-r)\frac{m^3}{\bar{\boldsymbol{u}}_f^2}, \tag{23}$$

which gives a non-linear equation for ρ upon substituting eq. (18) for ν_n.

5 The next steps

The previous sections outlined the essential features of a quasi-3D flow model that accounts for fluidization by the joint effect of dispersive pressure due to collisions between snow particles and excess pore pressure generated in the collapse of the snow cover under the weight of the avalanche. The following steps need to be carried out to fully implement the model:

- The pressure–density relation (1) ought to be tested for new snow from different climatic zones.

- Our proposed density–permeability relation for avalanches, eq. (8) in conjunction with eq. (6), also needs to be tested for its applicability. This is not easy, but can perhaps be achieved by measuring the density and permeability of avalanche deposits.
- The existing literature on the non-Darcian regime of flow through porous media needs to be investigated further to see whether suitable approximation formulas have been developed and experimentally verified. Alternatively, one may consider carrying out such tests on avalanche deposits or granular masses.
- If the extended NIS model is to be implemented, the full 3D formulation of the NIS model needs to be adapted to variable density. Moreover, the density dependence of the dispersive-stress coefficients generalizing ν_n and ν_s should be determined from 3D numerical simulations (or theoretical calculations if available).
- The conservation equations for mass and momentum should be adapted to include erosion.
- A maximally efficient method for solving the non-linear equation for the instantaneous density is crucial because that equation needs to be solved for each grid node at every time step.
- Due to high degree of non-linearity of the model equations, a robust numerical scheme is even more important than in simple models of the Voellmy type.

Experience with the block model implementation of the extended NIS model without seepage flow from the snow cover (Issler and Gauer, 2008) suggests that this model will mark a significant step forward, on the conceptual level and hopefully also on the practical level, once the challenges listed above are overcome.

References

Abele G and Gow AJ (1975) Compressibility characteristics of undisturbed snow. CRREL Research Report 336, U.S. Army Cold Regions Research and Engineering Laboratory, Hanover, New Hampshire, U.S.A.

Campbell CS and Gong A (1986) The stress-tensor in a two-dimensional granular shear flow. *J. Fluid Mech.*, **164**, 107–125

Carroll CS, Turnbull B and Louge MY (2012) Role of fluid density in shaping eruption currents driven by frontal particle blow-out. *Phys. Fluids*, **24**, 066603 (doi: 10.1063/1.4725538)

Carroll CS, Louge MY and Turnbull B (2013) Frontal dynamics of powder snow avalanches. *J. Geophys. Res.*, **118**(2), 913–924, ISSN 2169-9011 (doi: 10.1002/jgrf.20068)

Domine F, Morin S, Brun E, Lafaysse M and Carmagnola CM (2013) Seasonal evolution of snow permeability under equi-temperature and temperature-gradient conditions. *The Cryosphere*, **7**, 1915–1929

Gauer P and Issler D (2004) Possible erosion mechanisms in snow avalanches. *Annals Glaciol.*, **38**, 384–392

Issler D (2013) Snow avalanche dynamics—change and exchange. Talk presented at Fluid-Mediated Particle Transport in Geophysical Flows

Issler D (2014) Dynamically consistent entrainment laws for depth-averaged avalanche models. *J. Fluid Mech.*, **759**, 701–738 (doi: 10.1017/jfm.2014.584)

Issler D and Gauer P (2008) Exploring the significance of the fluidized flow regime for avalanche hazard mapping. *Annals Glaciol.*, **49**(1), 193–198, ISSN 02603055 (doi: 10.3189/172756408787814997)

Issler D, Jenkins JT and McElwaine JN (2017) Critique of avalanche flow models based on extensions of the concept of random kinetic energy. *J. Glaciol.*, **(to be submitted)**

Louge MY, Carroll CS and Turnbull B (2011) Role of pore pressure gradients in sustaining frontal particle entrainment in eruption currents: The case of powder snow avalanches. *J. Geophys. Res.*, **116**(F4), 002065 (doi: 10.1029/2011JF002065)

McElwaine J and Nishimura K (2001) Ping-pong ball avalanche experiments. *Annals Glaciol.*, **32**, 241–250

McElwaine JN (2005) Rotational flow in gravity current heads. *Phil. Trans. R. Soc. A*, **363**, 1603–1623 (doi: 10.1098/rsta.2005.1597)

McElwaine JN and Turnbull B (2005) Air pressure data from the Vallée de la Sionne avalanches of 2004. *J. Geophys. Res.*, **110**(F3), F03010; doi:10.1029/2004JF000237

Mellor M (1968) *Avalanches*. Number III-A3d in CRREL Monographs, U.S. Army Materiel Command, Cold Regions Research & Engineering Laboratory, Hanover, New Hampshire

Mellor M (1975) A review of basic snow mechanics. In *Snow Mechanics (Proceedings of the Grindelwald Symposium April 1974), IAHS Publ. no. 114*, 251–291, IAHS Press, Institute of Hydrology, Wallingford, Oxfordshire, UK

MiDi G (2004) On dense granular flows. *Eur. Phys. J. E*, **14**(4), 340–341 (doi: 10.1140/epje/i2003-10153-0)

Nishimura K, Sandersen F, Kristensen K and Lied K (1995) Measurements of powder snow avalanches –nature–. *Surv. Geophys.*, **16**, 649–660

Pasquarell GC, Ackermann NL, Shen HH and Hopkins MA (1988) Collisional stress in granular flows: Bagnold revisited. *J. Eng. Mech.*, **114**(1), 59–64 (doi: 10.1061/(ASCE)0733-9399(1988)114:1(49))

Shimizu H (1970) Air permeability of deposited snow. *Contrib. Inst. Low Temp. Sci.*, **A22**, 1–32

Steinkogler W, Sovilla B and Lehning M (2014) Influence of snow cover properties on avalanche dynamics. *Cold Regions Sci. Technol.*, **97**, 121–131 (doi: 10.1016/j.coldregions.2013.10.002)

Turnbull B and McElwaine JN (2008) Experiments on the non-Boussinesq flow of self-igniting suspension currents on a steep open slope. *J. Geophys. Res.*, **113**, F01003 (doi: 10.1029/2007JF000753)

Kontroll- og referanseside / Review and reference page

Dokumentinformasjon/*Document information*		
Dokumenttittel/*Document title* Notes on Fluidization of Snow Avalanches by Air Expulsion From the Snow Cover		**Dokumentnr./*Document no.*** 20140053-03-TN
Dokumenttype/*Type of document* Teknisk notat / *Technical note*	**Oppdragsgiver/*Client*** Norges vassdrags- og energidirektorat	**Dato/*Date*** 2017-02-03
Rettigheter til dokumentet iht kontrakt/*Proprietary rights to the document according to contract* ÅPEN: Skal tilgjengeliggjøres i åpent arkiv (BRAGE) / *OPEN: To be published in open archives (BRAGE)*		**Rev.nr. & dato/*Rev.no. & date*** 0 / 2017-02-03
Emneord/*Keywords* Snow avalanches, fluidization, snow cover, excess pore pressure		

Stedfesting/*Geographical information*	
Land, fylke/*Country* —	**Havområde/*Offshore area*** —
Kommune/*Municipality* —	**Feltnavn/*Field name*** —
Sted/*Location* —	**Sted/*Location*** —
Kartblad/*Map* —	**Felt, blokknr./*Field, Block No.*** —
UTM-koordinater/*UTM coordinates* **Sone:** 33N **Øst:** — **Nord:** —	**Koordinater/*Coordinates*** **Projeksjon, datum:** — **Øst:** ° ’ ” **Nord:** ° ’ ”

Dokumentkontroll/*Document control*
Kvalitetssikring i henhold til/*Quality assurance according to* NS-EN ISO9001

Rev.	**Revisjonsgrunnlag/*Reason for revision***	**Egenkontroll av/*Self review by:***	**Sidemanns-kontroll av/ *Colleague review by:***	**Uavhengig kontroll av/ *Independent review by:***	**Tverrfaglig kontroll av/ *Interdisciplinary review by:***
0	Originaldokument	Dieter Issler 2017-02-01	Peter Gauer 2017-02-03		

Dokument godkjent for utsendelse / *Document approved for release*	**Dato/*Date*** 2017-02-03	**Prosjektleder/*Project Manager*** Peter Gauer

NGI (Norges Geotekniske Institutt) er et internasjonalt ledende senter for forskning og rådgivning innen ingeniørrelaterte geofag. Vi tilbyr ekspertise om jord, berg og snø og deres påvirkning på miljøet, konstruksjoner og anlegg, og hvordan jord og berg kan benyttes som byggegrunn og byggemateriale.

Vi arbeider i følgende markeder: Offshore energi – Bygg, anlegg og samferdsel – Naturfare – Miljøteknologi.

NGI er en privat næringsdrivende stiftelse med kontor og laboratorier i Oslo, avdelingskontor i Trondheim og datterselskap i Houston, Texas, USA og i Perth, Western Australia.

www.ngi.no

NGI (Norwegian Geotechnical Institute) is a leading international centre for research and consulting within the geosciences. NGI develops optimum solutions for society and offers expertise on the behaviour of soil, rock and snow and their interaction with the natural and built environment.

NGI works within the following sectors: Offshore energy – Building, Construction and Transportation – Natural Hazards – Environmental Engineering.

NGI is a private foundation with office and laboratory in Oslo, branch office in Trondheim and daughter companies in Houston, Texas, USA and in Perth, Western Australia

www.ngi.no

OSLO
TRONDHEIM
HOUSTON
PERTH

NORGES GEOTEKNISKE INSTITUTT
NGI.NO

Hovedkontor Oslo
PB. 3930 Ullevål Stadion
0806 Oslo

Avd. Trondheim
PB. 5687 Sluppen
7485 Trondheim

T 22 02 30 00
F 22 23 04 48
NGI@ngi.no

BANK
KONTO 5096 05 01281
ORG.NR 958 254 318MVA

ISO 9001/14001
CERTIFIED BY BSI
FS 32989/EMS 612006